Detection and Segmentation of Ice Blocks in Europa's Chaos Terrain Using Mask R-CNN

Marina M. Dunn*
Bourns College of Engineering,
University of California, Riverside
Riverside, CA 92521 USA
marina.dunn@email.ucr.edu

Alyssa C. Mills
Department of Geosciences,
Baylor University
Waco, TX 76798 USA
alyssa_mills1@baylor.edu

Ahmed Awadallah
Southern Methodist University
Dallas, TX 75205 USA
ahmed.d8k8@gmail.com

Ethan J. Duncan
School of Information,
University of California, Berkeley
Berkeley, CA 94720 USA
ejduncan@asu.edu

Douglas M. Trent
Office of the Chief Information Officer,
NASA Langley Research Center
Hampton, VA 23666 USA
douglas.m.trent@nasa.gov

Andrew Larsen
Business Intelligence Division,
Inntopia
Stowe, VT 05672 USA
drewlarsen27@gmail.com

John Santerre
DeepLearning.AI
Palo Alto, CA 94306 USA
john.santerre@gmail.com

Conor A. Nixon
Planetary Systems Laboratory,
NASA Goddard Spaceflight Center
Greenbelt, MD 20771 USA
conor.a.nixon@nasa.gov

Abstract

The complex icy surface of Jupiter's moon, Europa, has long fascinated planetary science and astrobiology communities. NASA spacecraft observations of Europa have revealed an enigmatic chaos terrain, characterized by jigsaw-like areas of broken ice blocks caused by significant past subsurface disruption events. Speculation suggests the ice crust in these regions may be thinner, potentially offering better access to a warm ocean that may harbor complex organic compounds. These regions are favorable targets for future solar system missions, and may offer additional insight into Europa's internal processes. Although substantial progress has been made in visually cataloging chaos terrain, the precise mapping of ice blocks is laborious, subjective, and resource-intensive. Leveraging the capabilities of machine learning (ML) algorithms to expedite and automate such tasks will be crucial to scale this effort to other solar system bodies. To address this, we explore using a Mask R-CNN and transfer learning to detect and segment individual ice blocks within chaos terrain. Our current model achieves a highest precision score of 71.8% and recall score of 67.6%. We present the current strengths and limitations of our model and dataset while outlining avenues for further improvement. This work aims to contribute to future mission planning for Europa and other solar

*Corresponding author; marinadunn.github.io

Machine Learning and the Physical Sciences Workshop, NeurIPS 2023.

system bodies. Additionally, it highlights the unique algorithmic challenges posed by planetary science data and emphasizes the need for innovative ML solutions.

1 Introduction

Europa features a remarkably bright, relatively smooth icy surface [2, 6, 29, 47, 57, 21, 44, 11], and a subterranean ocean speculated to potentially host the ingredients for life [42, 37, 23]. Over the years, spacecraft missions like NASA's Pioneer 10 and 11 [16, 17], Voyager 1 and 2 [52, 51], Galileo [40], and Juno [36] have provided valuable imagery of the moon. Galileo was the first to unveil Europa's "chaos terrain" (example shown in Figure 1), where portions of ice crust fractured, drifted apart, rotated, and refroze [56, 9, 53, 45], resulting in elevated blocks amid an expanse of coarse, dull, "hummocky" matrix material, where original surface features are often obscured [9, 53, 20, 41, 39]. Remaining ice blocks exhibit distinct edges and morphologies ranging from large "plates" displaying textural evidence of preexisting terrain, to smaller "knobs" with less visible preexisting terrain features [21, 34]. Despite numerous formation hypotheses [22, 28, 12, 48, 15], no comprehensive model explains all observed instances of chaos terrain [34]. Although NASA's Juno spacecraft captured high-resolution surface imagery of Europa, it was not designed for extensive chaos terrain imaging; thus, Galileo observations remain the highest-quality available. Upcoming missions like NASA's Europa Clipper [30] and the European Space Agency's JUpiter Icy Moons Explorer (JUICE) [19] (both expected to arrive in 2030) will provide additional high-resolution surface imagery and enable a deeper geological analysis of features like chaos terrain, addressing remaining questions and enhancing understanding of their formation. These missions will also provide insight into physical properties like ice shell thickness and chemical composition, heat and material transport, etc.

Despite the recent emphasis on the need for machine learning (ML) in scientific research [13], a noticeable gap remains in ML-related publications, particularly at organizations like NASA, between planetary sciences and other fields such as heliophysics, astrophysics and Earth science [3]. As planetary science data volumes grow and demand for real-time spacecraft-based analysis rises, implementation of ML algorithms will be critical for driving scientific discoveries. Our approach seeks to maximize value for geoscientists by improving tracking of chaos ice block locations and orientations over time, and incorporating labels from domain experts who intend to extend these methods to unlabeled chaos regions.

2 Data

Our dataset utilizes regional mosaic maps ("RegMaps") of Europa's surface taken by the NASA Galileo Solid-State Imager (SSI) [5, 4] provided by the U.S. Geological Survey (USGS) Astrogeology Science Center, with resolutions ranging from 179-229 m/pixel [7]. Human labeling of ice blocks within chaos terrain is a nuanced task that considers factors like area, surface attributes, elevation, shape, etc. To ensure precise labeling and validation, we rely upon geoscientist expertise, incorporating georeferenced labels from chaos regions *Co*, *aa*, *bb*, *dd*, and *A-E* previously created by Leonard et al. [34], along with blocks from regions *ee*, *hh-kk*, and *F-I* labeled as part of Mills [38] following the same conventions. An unexpected mechanical failure with Galileo's high gain antenna restricted data transmission capabilities to only two low-gain antennas, resulting in reduced and low-resolution images [31]. Due to these spatial limitations, consequently only regions with total areas $\geq$1,500 km^2 that contain ice blocks $\geq$4 km^2 were selected for labeling. Furthermore, uncertainties in the spacecraft's position and orientation introduced significant errors in surface feature locations, causing misaligned images with displacement errors of up to 100 km [8]. In 2021, the USGS made extensive photogrammetric corrections to the dataset to mitigate issues and improve usability [8]. We have updated labels to account for these corrections. However, planetary science data still presents greater inherent data quality challenges than Earth-based or conventional remote sensing data, especially when contrasted with typical neural network training images. For instance, RegMaps still include shadows, varying solar angles, and diverse ice block morphologies. Coupled with limited data and increased object detection difficulty, these challenges pose a significant barrier to the effective application of deep learning algorithms in this domain.

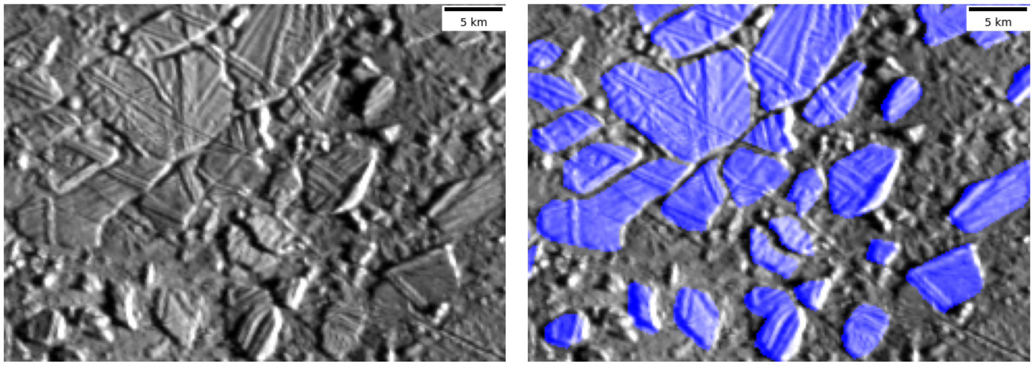

(a) Raw image (b) Ground truth labels included

Figure 1: Partial image of Conamara Chaos *Co*, without (a) and with (b) labels.

3 Methods

For the selection of our detection and segmentation model, we opted to employ a Mask Region-based Convolutional Neural Network (Mask R-CNN) framework [27], specifically built upon a ResNet50 backbone [26]. This choice was motivated by the framework's demonstrated robustness in various applications, making it well-suited for addressing the specific complexities of Europa's chaos ice blocks, and the fact that Mask R-CNN was still widely-favored framework for instance segmentation tasks within the scientific community at the time of initial project development. While more recent and sophisticated algorithms, such as those belonging to the YOLO family [10] or Transformer-based models [55], have since emerged, offering noteworthy advancements in capability, their implementation would have required a substantial expansion of the project's scope and likely necessitated additional computational resources that were unavailable. Given the existing funding constraints and organizational considerations, we chose to focus on a methodology that aligns with the project's initial objectives and resource availability. To overcome the inherent challenges of a small dataset, we implemented transfer learning by leveraging pre-trained statistical weights derived from the Common Objects in COntext (COCO) dataset [35]. This approach allowed us to fine-tune the model, adapting it to the unique characteristics of chaos terrain images, without the need for extensive labeled data specific to our target domain. We also used Leave-One-Out Cross-Validation (LOOCV) [25] to assess our model's performance.

We conducted pixel-level analyses for each chaos region, evaluating the overlap between ground truth and predicted segmentation masks. Initial pixel segmentation masks were generate from the georeferenced ice block labels. Training and test datasets were then created using overlapping, uniformly-sized image windows from RegMaps, ensuring that each window contains at least one label while removing cutoff labels. Hyperparameter optimization was executed using the Optuna framework [1] in two stages. An optimal minimum Intersection-over-Union (IoU) threshold score between 0.5 and 1 was first determined for each chaos region through a comprehensive sweep over the images. Subsequently, various objective functions were tested to maximize either average precision, recall, or F1 score calculated across all images. This structured setup revealed that maximizing the average F1 score yielded the most robust overall metrics. The identified optimal parameters included a learning rate of 0.001, batch size of 1, window crop size of 250x250 pixels, stride size of 64, utilization of the Adam optimizer [32], incorporation of 3 trainable backbone layers, setting a minimum area of 50 km^2 for an ice block to be considered valid, incorporation of horizontal and vertical random flips, and a final training duration of 15 epochs. Final segmentation maps were created by aggregating logits across the entire chaos region, maintaining the same crop size, stride, and score thresholds used during training. These predictions were then merged and superimposed onto the original RegMaps, resulting in georeferenced maps that can be used to determine the true coordinates and calculate areas for predicted ice blocks. This aspect holds particular significant value for geoscientists seeking precise measurements in their research.

4 Results and Discussion

Results for 250x250 images, including both pixel-wise and object-wise metric scores for each chaos region, are summarized in Table 1. Segmentation map predictions for regions *Co* and *gg* are illustrated in Figure 2. As anticipated, the model excels in Chaos *Co*, demonstrating robust performance in both pixel-level and object-level scores, attributed to higher image resolution and the prevalence of larger ice plates. Conversely, performance diminishes in regions with lower image resolutions, such as Chaos *aa*, *bb*, *ff*, and *gg*, and where ice plates are scarce, particularly in Chaos *D* and Chaos *E*. Additionally, the model frequently identifies analogous structures in areas beyond the boundaries of chaos terrain, including elevated surface features like "lineae" [14]. Similar challenges were observed in preliminary experiments with the recent Segment Anything model [33], exhibiting a tendency to indiscriminately detect various objects unrelated to chaos terrain. While this presents potential for broader geoscientific investigations, its effective integration would require more extensive modifications beyond the current project scope and chaos terrain focus.

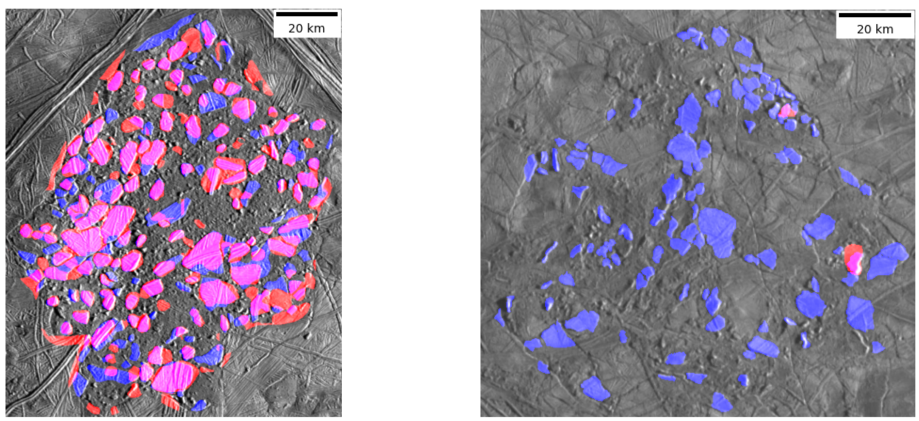

(a) Chaos *Co* (b) Chaos *gg*

Figure 2: Ground truth labels are in blue (false positives), model predictions (false negatives) are in red, and their overlaps (true positives) are in pink.

Variation in the model's successful identification of ice blocks is likely influenced by several factors. Notably, it could be attributed to lower phase angles in certain RegMap images, as these can impact image sharpness and texture. Expert labeling often requires adjustments like contrast stretching to enhance feature differentiation and visual interpretation. Similar adjustments applied to pixel-level maps may improve the model's predictions. Additionally, given that our image windows represent only small portions of complete RegMaps, and ice blocks are relatively small in size, precise edge demarcation can significantly affect all metrics. However, since our work is not primarily focused on exact edge testing, and we do not consider the original human labeling task to demand such a high degree of precision, it is unrealistic to expect the model to achieve this, and this aspect currently does not pertain directly to our core research question. Another concern arises from complexities introduced by partial objects during the windowing process. To mitigate irregular label cutoff at window edges, we implement a requirement that acceptable labels cannot occur along these edges. While this approach effectively addresses the issue in similar overlapping windowing scenarios, we recognize that different applications may necessitate alternative solutions. Given the overlapping nature of windows, it is expected and permissible for smaller ice blocks to appear in multiple training windows. However, this presents the challenge of smaller objects, like ice knobs, potentially overshadowing larger objects like ice plates in the training set, leading to misclassifications. This challenge is exacerbated in planetary science data collection during a flyby, where inherent variability in image scales results in pixels having different distance representations. To counter this, we employ a strategy of repeated inference on images, aggregating predictions and stitching them together into a single image. Additionally, although initial data augmentation attempts did not yield significant improvements, future exploration through detailed experiments is warranted for further refinement.

In contrast to an earlier study within our team led by Gansler et al. [18], which utilized Galileo imagery (pre-photogrammetric corrections release) and a U-Net framework [46] for semantic segmentation of ice blocks exclusively in the Conamara Chaos *Co* region, our current work implements a more

Region	Resolution (m/pix)	Pixel-Level			Object-Level		
		F1	Precision	Recall	F1	Precision	Recall
A	229	0.355	0.718	0.236	0.166	0.424	0.103
aa	210-222	0.001	0.027	0.001	0.000	0.000	0.000
B	229	0.367	0.489	0.293	0.152	0.500	0.090
bb	210-222	0.026	0.242	0.014	0.008	0.167	0.004
C	229	0.530	0.598	0.476	0.227	0.600	0.140
Co	179	0.642	0.612	0.676	0.568	0.618	0.526
D	229	0.305	0.268	0.354	0.105	0.208	0.070
dd	218	0.171	0.211	0.144	0.155	0.240	0.115
E	229	0.197	0.367	0.135	0.082	0.333	0.047
ee	210	0.400	0.367	0.436	0.286	0.357	0.238
F	215	0.328	0.323	0.333	0.223	0.353	0.158
ff	222	0.063	0.679	0.033	0.043	1.000	0.022
G	215	0.355	0.284	0.473	0.289	0.333	0.256
gg	222	0.036	0.553	0.018	0.000	0.000	0.000
H	215	0.110	0.066	0.326	0.089	0.080	0.100
hh	210	0.430	0.353	0.549	0.427	0.614	0.327
I	215	0.439	0.397	0.491	0.380	0.543	0.292
ii	210	0.496	0.454	0.546	0.411	0.443	0.384
jj	210	0.362	0.285	0.496	0.308	0.293	0.325
kk	210	0.415	0.321	0.587	0.333	0.348	0.320

Table 1: Complete LOOCV metric scores at the pixel and object level for 250x250 windows.

extensive approach. This makes direct comparisons challenging, especially given that the earlier approach achieved a maximum IoU score of only 0.286, and our study implemented a minimum IoU of 0.5 during threshold sweeps. Furthermore, a recent investigation by Haslebacher et al. [24] introduced *LineaMapper*, utilizing a similar Mask R-CNN setup for instance segmentation of four linear surface features using Europa Galileo imagery: "bands," "double ridges," "ridge complexes," and "undifferentiated lineae." *LineaMapper* achieved a highest precision score of 68% (for double ridges) and a highest recall score of 18% (for undifferentiated lineae), resulting in an average precision of 32% and average recall of 13% across all classes [24]. It's essential to note that while *LineaMapper* faced similar challenges with the Galileo dataset as our work, the broader global distribution of these linear features allowed for the utilization of additional high-resolution images, not available for chaos terrain, and a larger training dataset. While several other studies have focused on machine learning approaches for chaos terrain segmentation on other solar system bodies, such as Mars [49, 50], it is crucial to emphasize that these studies primarily pertain to rocky surfaces rather than icy crusts, which have vastly different geophysical contexts and implications. These distinctions underscore the unique complexities and limitations inherent in chaos terrain segmentation, emphasizing the necessity for cautious consideration when drawing comparisons.

5 Conclusion

Despite challenging data conditions, our approach demonstrates promise in detecting and segmenting ice blocks within Europa's chaos terrain. Nevertheless, we acknowledge the substantial room for improving performance metrics and refining our methodology. We plan to conduct additional experiments, exploring more advanced and powerful learning algorithms as alternatives to Mask R-CNN, and incorporating additional relevant datasets. Looking ahead, the anticipation of acquiring higher-resolution images from upcoming spacecraft missions holds considerable potential for enhancing overall segmentation model performance. We also recognize the importance of considering variables such as solar illumination angles and refining data augmentation techniques during future training processes. Our work not only highlights the invaluable role of machine learning in planetary science, but also serves as a foundational contribution to advancing our understanding of Europa's intriguing geophysical landscape.

6 Broader Impacts Statement

Our work strives to benefit geoscientists by streamlining the identification and tracking of ice blocks within Europa's chaos terrain and concurrently aims to advance the intersection of machine learning and physical sciences. Moreover, our work transcends its immediate domain by highlighting shared data challenges present across many STEM disciplines and emphasizing the need for tailored approaches. We emphasize that our approach is designed to complement geoscientist expertise, providing a powerful tool to support methodologies and reduce biases without replacing or undermining human knowledge. While we will continue to advocate for the adoption of similar machine learning approaches in interdisciplinary communities (i.e. astrobiology) within planetary science applications where we can contribute valuable insights, we believe it is also important to extend our work to the broader machine learning community in order to foster cross-disciplinary collaboration and garner sustained funding and support for future research endeavors. It's important to note that at its current stage, our project operates within the existing organizational funding and computational limitations. By sharing our research and preliminary findings with the broader machine learning community, we aim to underscore the potential impact of our work and lay the groundwork for renewed funding and support. This will enable us to conduct more comprehensive analyses and continue investigating additional machine learning approaches for similar problems. The authors of this tool are committed to deploying and implementing it responsibly, ethically and accessibly. Furthermore, we encourage the broader research community to scrutinize, build upon and improve our work, fostering collaboration across disciplines.

7 Data and Code Availability

The photogrammetrically-corrected Galileo SSI images used for labeling are publicly available through the USGS Astrogeology Science Center at https://doi.org/10.5066/P9VKKK7C. The labeled dataset used in this work from Mills [38] can be found at https://doi.org/10.5281/zenodo.10162452. These labels were created using the same conventions as Leonard et al. [34], but with corrected imagery [8]. The original dataset used in Leonard et al. [34] is publicly available at https://doi.org/10.5281/zenodo.6338798. The GitHub code repository for this research is available at https://github.com/marinadunn/europa-chaos-ML.

Computing Resources: Model development was conducted in a NASA-managed environment with Python 3 [54] and PyTorch [43] on Google Cloud, equipped with a NVIDIA Tesla T4 GPU.

8 Acknowledgments and Disclosure of Funding

We would like to thank Dr. Catherine C. Walker (Woods Hole Oceanographic Institution Department of Applied Ocean Physics and Engineering) and Dr. Rafael Augusto Pires de Lima (Department of Geography, University of Colorado, Boulder) for contributing their valuable Earth science-related expertise. We also thank Dr. Erin Leonard and Alyssa C. Mills for sharing chaos terrain labels used for model training, and Douglas M. Trent and David Na (NASA Headquarters) for providing the computing resources and data science support throughout this project. This material is based upon work supported by NASA under award number 80GSFC21M0002.

References

[1] T. Akiba, S. Sano, T. Yanase, T. Ohta, and M. Koyama. Optuna: A next-generation hyperparameter optimization framework. In *Proceedings of the 25th ACM SIGKDD International Conference on Knowledge Discovery and Data Mining*, page 2623–2631, Anchorage AK USA, Jul 2019. ACM. ISBN 978-1-4503-6201-6. doi: 10.1145/3292500.3330701. URL https://dl.acm.org/doi/10.1145/3292500.3330701.

[2] C. Alexander, R. Carlson, G. Consolmagno, R. Greeley, and D. Morrison. *The Exploration History of Europa*, page 3–26. University of Arizona Press, 2009. ISBN 978-0-8165-3851-5. doi: 10.2307/j.ctt1xp3wdw.7. URL https://www.jstor.org/stable/j.ctt1xp3wdw.7.

[3] A. Azari, J. B. Biersteker, R. M. Dewey, G. Doran, E. J. Forsberg, C. D. K. Harris, H. R. Kerner, K. A. Skinner, A. W. Smith, R. Amini, S. Cambioni, V. D. Poian, T. M. Garton, M. D. Himes, S. Millholland, and S. Ruhunusiri. Integrating Machine Learning for Planetary Science: Perspectives for the Next Decade. *Bulletin of the AAS*, 53(4), Mar 2021. doi: 10.3847/25c2cfeb.aa328727. URL https://baas.aas.org/pub/2021n4i128.

[4] M. J. Belton, J. W. Head, A. P. Ingersoll, R. Greeley, A. S. McEwen, K. P. Klaasen, D. Senske, R. Pappalardo, G. Collins, A. R. Vasavada, and et al. Galileo's First Images of Jupiter and the Galilean Satellites. *Science*, 274(5286):377–385, Oct 1996. doi: 10.1126/science.274.5286.377.

[5] M. J. S. Belton, K. P. Klaasen, M. C. Clary, J. L. Anderson, C. D. Anger, M. H. Carr, C. R. Chapman, M. E. Davies, R. Greeley, D. Anderson, L. K. Bolef, T. E. Townsend, R. Greenberg, J. W. Head, G. Neukum, C. B. Pilcher, J. Veverka, P. J. Gierasch, F. P. Fanale, A. P. Ingersoll, H. Masursky, D. Morrison, and J. B. Pollack. The Galileo Solid-State Imaging Experiment. *Space Science Reviews*, 60(1–4):413–455, May 1992. ISSN 0038-6308, 1572-9672. doi: 10.1007/BF00216864. URL https://link.springer.com/10.1007/BF00216864.

[6] E. B. Bierhaus, K. Zahnle, and C. R. Chapman. *Europa's Crater Distributions and Surface Ages*, page 161–180. University of Arizona Press, 2009. ISBN 978-0-8165-3851-5. URL https://www.jstor.org/stable/j.ctt1xp3wdw.13. page: 161 container-title: Europa ADS Bibcode: 2009euro.book..161B.

[7] M. T. Bland. Photogrammetrically Controlled, Equirectangular Galileo Image Mosaics of Europa, 2021. URL https://astrogeology.usgs.gov/search/map/Europa/Mosaic/Equirectangular_Mosaics_of_Europa_v3.

[8] M. T. Bland, L. A. Weller, B. A. Archinal, E. Smith, and B. H. Wheeler. Improving the Usability of Galileo and Voyager Images of Jupiter's Moon Europa. *Earth and Space Science*, 8(12), Oct 2021. doi: 10.1029/2021ea001935.

[9] M. H. Carr, M. J. Belton, C. R. Chapman, M. E. Davies, P. Geissler, R. Greenberg, A. S. McEwen, B. R. Tufts, R. Greeley, R. Sullivan, and et al. Evidence for a Subsurface Ocean on Europa. *Nature*, 391(6665): 363–365, 1998. doi: 10.1038/34857.

[10] Y. W. Chen and J. M. Shiu. An implementation of yolo-family algorithms in classifying the product quality for the acrylonitrile butadiene styrene metallization. *The International Journal of Advanced Manufacturing Technology*, 119(11–12):8257–8269, April 2022. ISSN 0268-3768, 1433-3015. doi: 10.1007/s00170-022-08676-5. URL https://link.springer.com/10.1007/s00170-022-08676-5.

[11] G. Collins and F. Nimmo. Chaotic Terrain on Europa. In *Europa*, page 259–282. University of Arizona Press, 2009. ISBN 978-0-8165-3851-5. doi: 10.2307/j.ctt1xp3wdw. URL https://doi.org/10.2307/j.ctt1xp3wdw.17.

[12] G. C. Collins, J. W. Head, R. T. Pappalardo, and N. A. Spaun. Evaluation of Models for the Formation of Chaotic Terrain on Europa. *Journal of Geophysical Research: Planets*, 105(E1):1709–1716, Jan 2000. ISSN 01480227. doi: 10.1029/1999JE001143. URL https://doi.wiley.com/10.1029/1999JE001143.

[13] Committee on the Planetary Science, Astrobiology Decadal Survey, Space Studies Board and Division on Engineering and Physical Sciences, and National Academies of Sciences, Engineering and Medicine. *Origins, Worlds, and Life: A Decadal Strategy for Planetary Science and Astrobiology 2023-2032*. National Academies Press, Washington, D.C., 2022. ISBN 978-0-309-47578-5. doi: 10.17226/26522. URL https://nap.nationalacademies.org/catalog/26522.

[14] M. E. Davies. *Cartography and Nomenclature for the Galilean Satellites*. University of Arizona Press, Jan 1982. URL https://ui.adsabs.harvard.edu/abs/1982stjp.conf..911D.

[15] P. H. Figueredo and R. Greeley. Resurfacing History of Europa from Pole-to-pole Geological Mapping. *Icarus*, 167(2):287–312, Feb 2004. ISSN 00191035. doi: 10.1016/j.icarus.2003.09.016. URL https://linkinghub.elsevier.com/retrieve/pii/S0019103503002938.

[16] R. O. Fimmel, W. Swindell, and E. Burgess. *Pioneer Odyssey*. Scientific and Technical Information Office, National Aeronautics and Space Administration, Washington, D.C., 1977.

[17] R. O. Fimmel, J. Van Allen, and E. Burgess. *Pioneer: First to Jupiter, Saturn, and Beyond*. Scientific and Technical Information Office, National Aeronautics and Space Administration, Washington, D.C., 1980. ISBN 978-99973-982-5-3.

[18] K. Gansler, C. Liles, and C. Nixon. Using Machine Learning to Detect Chaos Terrain on Europa. In *AGU Fall Meeting Abstracts*, volume 2021, pages P11B–11, Dec. 2021.

[19] O. Grasset, M. Dougherty, A. Coustenis, E. Bunce, C. Erd, D. Titov, M. Blanc, A. Coates, P. Drossart, L. Fletcher, and et al. Jupiter Icy Moons Explorer (JUICE): An ESA mission to Orbit Ganymede and to Characterise the Jupiter system. *Planetary and Space Science*, 78:1–21, 2013. doi: 10.1016/j.pss.2012.12.002.

[20] R. Greeley. *Geology of Europa: Galileo Update*, volume 220 of *Astrophysics and Space Science Library*, page 191–200. Springer Netherlands, Dordrecht, 1997. ISBN 978-90-481-4955-1. doi: 10.1007/978-94-015-8790-7_15. URL https://link.springer.com/10.1007/978-94-015-8790-7_15.

[21] R. Greeley, P. H. Figueredo, D. A. Williams, F. C. Chuang, J. E. Klemaszewski, S. D. Kadel, L. M. Prockter, R. T. Pappalardo, J. W. Head, G. C. Collins, N. A. Spaun, R. J. Sullivan, J. M. Moore, D. A. Senske, B. R. Tufts, T. V. Johnson, M. J. S. Belton, and K. L. Tanaka. Geologic Mapping of Europa. *Journal of Geophysical Research: Planets*, 105(E9):22559–22578, Sep 2000. ISSN 01480227. doi: 10.1029/1999JE001173. URL https://doi.wiley.com/10.1029/1999JE001173.

[22] R. Greenberg, S. Kadel, J. Riley, P. Geissler, B. R. Tufts, and G. V. Hoppa. Chaos on Europa. *Icarus*, 141 (2):263–286, 1999. doi: https://doi.org/10.1006/icar.1999.6187.

[23] K. P. Hand, C. F. Chyba, J. C. Priscu, R. W. Carlson, and K. H. Nealson. *Astrobiology and the Potential for Life on Europa*, page 589–630. University of Arizona Press, 2009. ISBN 978-0-8165-3851-5. URL https://www.jstor.org/stable/j.ctt1xp3wdw.32.

[24] C. Haslebacher, N. Thomas, and V. T. Bickel. Lineamapper: A deep learning-powered tool for mapping linear surface features on europa. *Icarus*, page 115722, Jul 2023. ISSN 00191035. doi: 10.1016/j.icarus.2023.115722. URL https://linkinghub.elsevier.com/retrieve/pii/S0019103523002993.

[25] T. Hastie, R. Tibshirani, and J. Friedman. *The Elements of Statistical Learning*. Springer Series in Statistics. Springer New York, New York, NY, 2009. ISBN 978-0-387-84857-0. doi: 10.1007/978-0-387-84858-7. URL https://link.springer.com/10.1007/978-0-387-84858-7.

[26] K. He, X. Zhang, S. Ren, and J. Sun. Deep Residual Learning for Image Recognition. In *2016 IEEE Conference on Computer Vision and Pattern Recognition (CVPR)*, page 770–778. IEEE, June 2016. ISBN 978-1-4673-8851-1. doi: 10.1109/CVPR.2016.90. URL https://ieeexplore.ieee.org/document/7780459/.

[27] K. He, G. Gkioxari, P. Dollár, and R. Girshick. Mask r-cnn. In *2017 IEEE International Conference on Computer Vision (ICCV)*, pages 2980–2988, 2017. doi: 10.1109/ICCV.2017.322. URL https://ieeexplore.ieee.org/document/8237584.

[28] J. W. Head, R. T. Pappalardo, and R. Sullivan. Europa: Morphological Characteristics of Ridges and Triple Bands from Galileo Data (E4 and E6) and Assessment of a Linear Diapirism Model. *Journal of Geophysical Research: Planets*, 104(E10):24223–24236, Oct 1999. ISSN 01480227. doi: 10.1029/1998JE001011. URL https://doi.wiley.com/10.1029/1998JE001011.

[29] S. M. Howell and R. T. Pappalardo. Can earth-like plate tectonics occur in ocean world ice shells? *Icarus*, 322:69–79, Apr 2019. ISSN 00191035. doi: 10.1016/j.icarus.2019.01.011. URL https://linkinghub.elsevier.com/retrieve/pii/S001910351830407X.

[30] S. M. Howell and R. T. Pappalardo. NASA's Europa Clipper— A Mission to a Potentially Habitable Ocean World. *Nature Communications*, 11(1), Mar 2020. doi: 10.1038/s41467-020-15160-9.

[31] M. R. Johnson. The Galileo High Gain Antenna Deployment Anomaly. In *28th Aerospace Mechanisms Symposium, NASA CP-3260*, page 359–377, Cleveland, OH, USA, May 1994. NASA Lewis Research Center. URL https://ntrs.nasa.gov/citations/19940028813.

[32] D. P. Kingma and J. Ba. Adam: A method for stochastic optimization. In *Proceedings of the 3rd International Conference on Learning Representations*, San Diego, CA, USA, 2015. arXiv. doi: 10.48550/ARXIV.1412.6980. URL https://arxiv.org/abs/1412.6980.

[33] A. Kirillov, E. Mintun, N. Ravi, H. Mao, C. Rolland, L. Gustafson, T. Xiao, S. Whitehead, A. C. Berg, W.-Y. Lo, P. Dollár, and R. Girshick. Segment anything. *ArXiv*, abs/2304.02643, 2023. doi: 10.48550/ARXIV.2304.02643. URL https://arxiv.org/abs/2304.02643.

[34] E. J. Leonard, S. M. Howell, A. Mills, D. A. Senske, D. A. Patthoff, H. C. F. C. Hay, and R. T. Pappalardo. Finding Order in Chaos: Quantitative Predictors of Chaos Terrain Morphology on Europa. *Geophysical Research Letters*, 49(8):e2021GL097309, 2022. doi: https://doi.org/10.1029/2021GL097309. URL https://agupubs.onlinelibrary.wiley.com/doi/abs/10.1029/2021GL097309.

[35] T. Lin, M. Maire, S. J. Belongie, L. D. Bourdev, R. B. Girshick, J. Hays, P. Perona, D. Ramanan, P. Doll'a r, and C. L. Zitnick. Microsoft COCO: Common Objects in Context. *CoRR*, abs/1405.0312, 2014. URL https://arxiv.org/abs/1405.0312.

[36] S. Matousek. The Juno New Frontiers Mission. In *56th International Astronautical Congress of the International Astronautical Federation, the International Academy of Astronautics, and the International Institute of Space Law*, Fukuoka, Japan, Oct 2005. American Institute of Aeronautics and Astronautics. doi: 10.2514/6.IAC-05-A3.2.A.04. URL https://arc.aiaa.org/doi/10.2514/6.IAC-05-A3.2.A.04.

[37] W. B. McKinnon, R. T. Pappalardo, and K. K. Khurana. *Europa: Perspectives on an Ocean World*, page 697–710. University of Arizona Press, 2009. ISBN 978-0-8165-3851-5. URL https://www.jstor.org/stable/j.ctt1xp3wdw.35.

[38] A. C. Mills. Europa Chaos Block Shapefiles and Geojson Files in Lower RegMap Images. https://doi.org/10.5281/zenodo.10162452, Nov 2023. URL https://doi.org/10.5281/zenodo.10162452.

[39] C. Neish, L. Prockter, and G. W. Patterson. The Identification of Chaotic Terrain on Europa. In *EPSC-DPS Joint Meeting 2011*, volume 2011, page 259, Oct 2011.

[40] W. J. O'Neill and R. T. Mitchell. Galileo Mission Overview. In *21st Aerospace Sciences Meeting*, Reno, Nevada, USA, Jan 1983. American Institute of Aeronautics and Astronautics. doi: https://doi.org/10.2514/6.1983-96. URL https://arc.aiaa.org/doi/abs/10.2514/6.1983-96.

[41] R. T. Pappalardo, J. W. Head, R. Greeley, R. J. Sullivan, C. Pilcher, G. Schubert, W. B. Moore, M. H. Carr, J. M. Moore, M. J. S. Belton, and D. L. Goldsby. Geological Evidence for Solid-state Convection in Europa's Ice Shell. *Nature*, 391(6665):365–368, Jan. 1998. ISSN 0028-0836, 1476-4687. doi: 10.1038/34862. URL https://www.nature.com/articles/34862.

[42] R. T. Pappalardo, M. J. S. Belton, H. H. Breneman, M. H. Carr, C. R. Chapman, G. C. Collins, T. Denk, S. Fagents, P. E. Geissler, B. Giese, R. Greeley, R. Greenberg, J. W. Head, P. Helfenstein, G. Hoppa, S. D. Kadel, K. P. Klaasen, J. E. Klemaszewski, K. Magee, A. S. McEwen, J. M. Moore, W. B. Moore, G. Neukum, C. B. Phillips, L. M. Prockter, G. Schubert, D. A. Senske, R. J. Sullivan, B. R. Tufts, E. P. Turtle, R. Wagner, and K. K. Williams. Does europa have a subsurface ocean? evaluation of the geological evidence. *Journal of Geophysical Research: Planets*, 104(E10):24015–24055, Oct 1999. ISSN 0148-0227. doi: 10.1029/1998JE000628. URL https://agupubs.onlinelibrary.wiley.com/doi/10.1029/1998JE000628.

[43] A. Paszke, S. Gross, F. Massa, A. Lerer, J. Bradbury, G. Chanan, T. Killeen, Z. Lin, N. Gimelshein, L. Antiga, A. Desmaison, A. Köpf, E. Yang, Z. DeVito, M. Raison, A. Tejani, S. Chilamkurthy, B. Steiner, L. Fang, J. Bai, and S. Chintala. PyTorch: An Imperative Style, High-Performance Deep Learning Library. In *33rd Conference on Neural Information Processing Systems*, page 8024–8035, Vancouver, Canada, 2019. URL https://proceedings.neurips.cc/paper_files/paper/2019/file/bdbca288fee7f92f2bfa9f7012727740-Paper.pdf.

[44] L. M. Prockter and G. W. Patterson. *Morphology and Evolution of Europa's Ridges and Bands*, page 237–258. University of Arizona Press, 2009. ISBN 978-0-8165-3851-5. URL https://www.jstor.org/stable/j.ctt1xp3wdw.16.

[45] L. M. Prockter, A. M. Antman, R. T. Pappalardo, J. W. Head, and G. C. Collins. Europa: Stratigraphy and Geological History of the Anti-Jovian Region from Galileo E14 Solid-state Imaging Data. *Journal of Geophysical Research: Planets*, 104(E7):16531–16540, Jul 1999. ISSN 01480227. doi: 10.1029/1998JE001015. URL https://doi.wiley.com/10.1029/1998JE001015.

[46] O. Ronneberger, P. Fischer, and T. Brox. U-Net: Convolutional Networks for Biomedical Image Segmentation. *Lecture Notes in Computer Science*, 9351:234–241, Nov 2015. doi: 10.1007/978-3-319-24574-4_28.

[47] P. M. Schenk, C. R. Chapman, K. Zahnle, and J. M. Moore. *Ages and interiors: the cratering record of the Galilean satellites*, volume 1, page 427–456. Cambridge University Press, 2004. ISBN 978-0-521-81808-7. URL https://ui.adsabs.harvard.edu/abs/2004jpsm.book..427S.

[48] B. E. Schmidt, D. D. Blankenship, G. W. Patterson, and P. M. Schenk. Active Formation of 'Chaos Terrain' Over Shallow Subsurface Water on Europa. *Nature*, 479(7374):502–505, Nov. 2011. ISSN 0028-0836, 1476-4687. doi: 10.1038/nature10608. URL https://www.nature.com/articles/nature10608.

[49] H. Shozaki, Y. Sekine, and N. Guttenberg. Classification of Martian Chaos Terrains Using Imagery Machine Learning: Implications for Ground Ice Distributions and Dynamics. In *American Geophysical Union, Fall Meeting 2020*, volume 2020, pages P042–0011, Dec. 2020. URL https://ui.adsabs.harvard.edu/abs/2020AGUFMP042.0011S. ADS Bibcode: 2020AGUFMP042.0011S.

[50] H. Shozaki, Y. Sekine, N. Guttenberg, and G. Komatsu. Recognition and Classification of Martian Chaos Terrains Using Imagery Machine Learning: A Global Distribution of Chaos Linked to Groundwater Circulation, Catastrophic Flooding, and Magmatism on Mars. *Remote Sensing*, 14(16):3883, Aug 2022. ISSN 2072-4292. doi: 10.3390/rs14163883. URL https://www.mdpi.com/2072-4292/14/16/3883.

[51] B. A. Smith, L. A. Soderblom, R. Beebe, J. Boyce, G. Briggs, M. Carr, S. A. Collins, A. F. Cook, G. E. Danielson, M. E. Davies, and et al. The Galilean Satellites and Jupiter: Voyager 2 Imaging Science Results. *Science*, 206(4421):927–950, Nov 1979. doi: 10.1126/science.206.4421.927.

[52] B. A. Smith, L. A. Soderblom, T. V. Johnson, A. P. Ingersoll, S. A. Collins, E. M. Shoemaker, G. E. Hunt, H. Masursky, M. H. Carr, M. E. Davies, and et al. The Jupiter System Through the Eyes of Voyager 1. *Science*, 204(4396):951–972, Jun 1979. doi: 10.1126/science.204.4396.951.

[53] N. A. Spaun, J. W. Head, G. C. Collins, L. M. Prockter, and R. T. Pappalardo. Conamara Chaos Region, Europa: Reconstruction of Mobile Polygonal Ice Blocks. *Geophysical Research Letters*, 25(23):4277–4280, 1998. doi: https://doi.org/10.1029/1998GL900176. URL https://agupubs.onlinelibrary.wiley.com/doi/abs/10.1029/1998GL900176.

[54] G. Van Rossum and F. L. Drake. *Python 3 Reference Manual*. CreateSpace, Scotts Valley, CA, 2009. ISBN 1441412697.

[55] A. Vaswani, N. Shazeer, N. Parmar, J. Uszkoreit, L. Jones, A. N. Gomez, L. Kaiser, and I. Polosukhin. Attention is all you need. In I. Guyon, U. V. Luxburg, S. Bengio, H. Wallach, R. Fergus, S. Vishwanathan, and R. Garnett, editors, *Advances in Neural Information Processing Systems 30 (NIPS 2017)*, volume 30, Long Beach, CA, USA, 2017. ISBN 978-1-5108-6096-4. URL https://proceedings.neurips.cc/paper_files/paper/2017/file/3f5ee243547dee91fbd053c1c4a845aa-Paper.pdf.

[56] K. K. Williams and R. Greeley. Estimates of Ice Thickness in the Conamara Chaos Region of Europa. *Geophysical Research Letters*, 25(23):4273–4276, 1998. doi: https://doi.org/10.1029/1998GL900144. URL https://agupubs.onlinelibrary.wiley.com/doi/abs/10.1029/1998GL900144.

[57] K. Zahnle, P. Schenk, H. Levison, and L. Dones. Cratering rates in the outer solar system. *Icarus*, 163 (2):263–289, Jun 2003. ISSN 00191035. doi: 10.1016/S0019-1035(03)00048-4. URL https://linkinghub.elsevier.com/retrieve/pii/S0019103503000484.

A Supplementary Material

A.1 Additional Model Training Information

Hyperparameter	Min	Max	Final
Crop Size	128	512	250
Stride	8	128	64
Batch Size	1	8	1
Trainable Backbone Layers	0	5	3
Learning Rate	0.01	0.0001	0.001
Optimizer	ADAM	SGD	ADAM
Epochs	1	50	15

Table 2: Optuna hyperparameter search specifications.

Region	Plates	Knobs	Total Objects	Region Area (km^2)	Lon (°)	Lat (°)	Mosaic ID	Resolution (m/pixel)
aa	31	176	207	13151.6	129.63	9.42	17ESREGMAP01 17ESNERTRM01 11ESREGMAP01	210 218 222
bb	91	221	312	22553	128.42	1.32	17ESREGMAP01 17ESNERTRM01 11ESREGMAP01	210 218 222
Co	149	6	155	9020.9	86.65	9.66	E6ESDRKLIN01	179
dd	23	31	54	7965.5	125.38	3.64	11ESREGMAP01	218
ee	9	34	43	3127	131.26	-17.33	17ESNERTRM01	210
ff	23	24	47	2299.1	143.5	-23.41	17ESREGMAP01	222
gg	62	49	111	7750.2	141.83	-26.28	17ESREGMAP01	222
hh	38	70	108	6036.5	139.78	-36.17	17ESNERTRM01	210
ii	44	108	152	11718.4	137.01	-39.41	17ESNERTRM01	210
jj	31	48	79	6921.4	140.1	-41.28	17ESNERTRM01	210
kk	8	23	31	1787.6	137.12	-42.59	17ESNERTRM01	210
A	59	184	243	12255.3	-84.62	34.41	15ESREGMAP02	229
B	18	72	90	2761.3	-78.82	30.68	15ESREGMAP02	229
C	45	42	87	2936.8	-79.36	25.65	15ESREGMAP02	229
D	2	70	72	1953.7	73.95	25.66	15ESREGMAP02	229
E	3	84	87	7665.5	-82.59	22.41	15ESREGMAP02	229
F	14	27	41	2912.9	-75.28	-19.88	17ESREGMAP02	215
G	19	19	38	4286.6	-73.16	-21.25	17ESREGMAP02	215
H	5	15	20	2237.4	-70.99	-21.26	17ESREGMAP02	215
I	38	29	67	5923.9	-81.44	-30.66	17ESREGMAP02	215

Table 3: Ground truth label object counts and total region areas, and USGS Galileo SSI mosaic IDs with corresponding image resolutions, for each Europa chaos region used during model training.